Editors' Suggestion | Featured in Physics

Rheology of Entangled Active Polymer-Like *T. Tubifex* Worms

A. Deblais,[1,*] S. Woutersen,[2,†] and D. Bonn[1,‡]

[1]*Van der Waals-Zeeman Institute, Institute of Physics, University of Amsterdam, 1098XH Amsterdam, The Netherlands*

[2]*Van 't Hoff Institute for Molecular Sciences, University of Amsterdam, Science Park 904, 1098XH Amsterdam, The Netherlands*

(Received 18 November 2019; revised manuscript received 18 March 2020; accepted 13 April 2020; published 8 May 2020)

We experimentally study the rheology of long, slender, and entangled living worms (*Tubifex Tubifex*). Their level of activity can be controlled by changing the temperature or by adding small amounts of alcohol to make the worms temporarily inactive. Performing classical rheology experiments on this entangled polymer-like system, we find that the rheology is qualitatively similar to that of usual polymers, but, quantitatively, (i) shear thinning is reduced by activity, (ii) the characteristic shear rate for the onset of shear-thinning is given by the time scale of the activity, and (iii) the low shear viscosity as a function of concentration shows a very different scaling from that of regular polymers. Our study paves the way towards a new experimental research field of active "polymer-like worms."

DOI: 10.1103/PhysRevLett.124.188002

Of all complex fluids, it is probably the rheology of polymers we understand best. In certain limits it is possible to predict for instance the shear-thinning rheology and the behavior in other flow situations of practical importance such as elongation [1]. The situation is markedly different when we move from *passive* [2,3] to *active* polymers where the coupling of filament activity, hydrodynamic interactions, and conformations open the way to a plethora of novel structural and dynamical features [4–10]. Active systems consist of interacting agents that are able to extract energy from the environment to produce sustained motion [5]. The local conversion of energy into mechanical work drives the system far from equilibrium, yielding new dynamics and phases [11–14]. Understanding the nonequilibrium statistical mechanics of such active systems is a major challenge, both experimentally and theoretically. While theoretically, much progress has been made recently, the number of experimental systems is still very limited [4,15–21] and often restricted to a relatively small number of simple entities such as driven colloidal particles [22–24].

We study here the collective rheological behavior of a system that is active and in structure greatly resembles polymer solutions and melts, a system eminently adapted to a statistical mechanical description that typically forms the basis of polymer models. *Tubifex Tubifex* worms [25], also called sludge worms, represent a simple and affordable system to study active polymer rheology. The worms are readily available in large quantities: they are commonly used as food for aquarium fish, and are available in most pet shops. They are active swimmers and have a typical length of 10–30 mm and width of 0.2–0.4 mm [26]. When randomly distributed over a volume of water, the worms exhibit random motion and form highly entangled "blobs" [29] [see inset of Fig. 1(a)].

In order to compare our living worms with active polymers, we first focus on a well-known phenomenon in polymer flows, which is that of shear thinning. Shear thinning is a reflection of the orientation of chain segments, and not necessarily changes in the overall size and shape of coils; however, in many cases the segment orientation does follow the coil-level behavior. It is due to fact that the thermal fluctuations of polymer chains tend to randomize their conformation, while the flow tends to orient and stretch them. The higher the flow rate, the more oriented the polymers, and the smaller the flow resistance, as is observed for instance in wormlike micellar solutions [30]; however, unlike some concentrated wormlike micellar

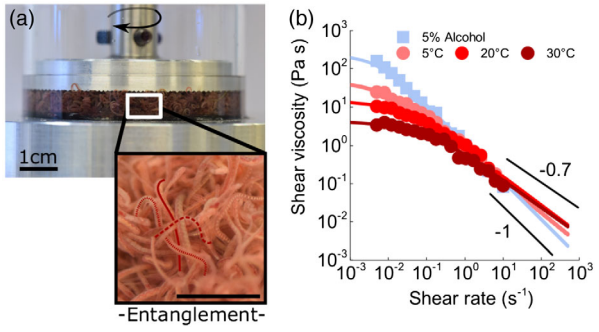

FIG. 1. Rheology experiments of polymer-like worms. (a) Picture of the custom-designed rheology cell (see Supplemental Video 1 [26]) used for the measurements. The cell is mounted on a Peltier cell to control the *in situ* temperature T and thus the level of activity of the worms. The enlargement emphasizes the entangled state of the worms. (b) Shear-thinning curves (shear viscosity η_s as a function of shear rate $\dot{\gamma}$) of the polymer-like solution ($\phi = 28\%_{\mathrm{vol}}$) at different levels of activity, as tuned by adding 5% of alcohol and varying the temperature ($T = 5, 20, 30\,^{\circ}\mathrm{C}$). Colored solid lines are fits to the Cross model (1).

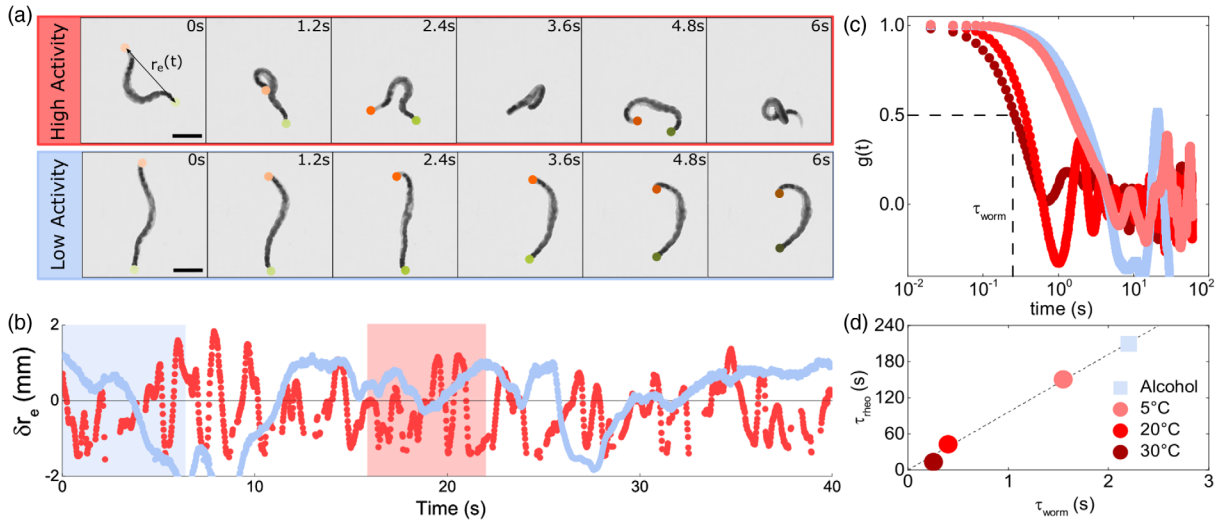

FIG. 2. Microscopic dynamics of a single worm. (a) Sequence of images (initially recorded at a rate of 50 frames per second) of a single worm at a high level of activity in water at $T = 30\,^{\circ}\mathrm{C}$ constrained to move in a quasi-two-dimensional thermo-controlled aquarium. Similar analysis as in the higher panel for the same worm at a lower level of activity, achieved by lowering the temperature to $T = 20\,^{\circ}\mathrm{C}$ and exposing the worm to 5% of alcohol. (b) Corresponding plot of the fluctuation of the end-to-end distance δr_e with respect to its averaged value versus time. Scale bar in the sequence of images represents 2 mm. The red shaded area in the plot indicates the six-second time period during which the sequence of images shown in the top panel were recorded. (c) Autocorrelation function of $\delta(r_e)$ measured at different levels of activity (i.e., different temperatures $T = 5$, 20, $30\,^{\circ}\mathrm{C}$ and in the presence of alcohol). From these graphs, the (microscopic) characteristic time τ_{worm} of a single worm was determined as indicated by the dotted lines. (d) Characteristic time of the active solution as deduced from rheology τ_{rheo} plotted against the (microscopic) characteristic time τ_{worm} of a single worm at four levels of activity. The dashed line is a linear fit of the data.

systems we do not observe shear thickening. Shear thinning can also be due to entangled polymer chains getting disentangled as a result of the flow, again resulting in increased orientation and hence a smaller flow resistance with increasing shear rate. In the context of out-of-equilibrium materials, recent experimental works evidence that cycles of assembly and disassembly of bonds between active constituents lead to stress relaxation [21,31].

We qualitatively study the effect of activity on the shear thinning of the polymer-like worms by performing rheology experiments in a custom-designed plate-plate geometry (Fig. 1, [26]). A known mass of *Tubifex* is mixed with different amounts of (tap) water to adjust the polymer concentration, corresponding to an effective volume fraction $\phi = V_{\mathrm{worm}}/V_{\mathrm{tot}}$, where $V_{\mathrm{worm}} = \rho_{\mathrm{worm}}/m_{\mathrm{worm}}$, $V_{\mathrm{tot}} = V_{\mathrm{worm}} + V_{\mathrm{water}}$, m_{worm} is the mass of worms added in the rheology cell and $\rho_{\mathrm{worm}} = 1.05\ \mathrm{g\ cm^{-3}}$ is the averaged density of a worm. We put them in a beaker with a rough bottom that fits on the rheometer. By inserting an equally rough top plate that just fits into the beaker, we create a plate-plate geometry in which the polymer-like worms are confined and rheology experiments can be performed. By this means and with the help of the transparent glass window of the geometry we can visually confirm that the worm dispersion remains homogeneous whilst continuously shearing (Supplemental Video 1 [26]). This is also confirmed by the flow curves; if sedimentation would affect the measurement, it would introduce a yield stress in the flow curves as reported in [32] for a hard-particle suspension, which we do not observe. At the shear rates probed here, resuspension is thus more efficient than sedimentation. We also checked possible effects of slippage on the velocity profiles for 3 different shear rates covering the range of shear rates studied (0.1, 0.5, and 1 $\mathrm{s^{-1}}$); flow field measurements reveal that the shear profiles are quasi independent of the shear rate; the apparent shear rates are found to be ~2 times smaller than the applied ones indicating a significant amount of slip near the top plate [26]. We correct all the values of the shear rates accordingly.

The setup as a whole is thermostated using Peltier elements, allowing us to control the polymer activity by changing the temperature T (Fig. 2). An efficient way to suppress the activity of the worms is to add 5% alcohol to the water, which causes almost all of the activity to cease [33], impacting their random motion in a similar fashion [26,29]. This is reversible: if the alcohol is rinsed away using tap water, the activity returns (Supplemental Video 2 [26]). In Fig. 1(b) we compare the rheology of a solution of active worms ($\phi = 28\%_{\mathrm{vol}}$, $T = 20\,^{\circ}\mathrm{C}$) to that of the same solution rendered inactive by adding 5% alcohol or lowering the temperature. We find that the shear-thinning behavior is strongly attenuated by activity. Adding the alcohol (or lowering the temperature) causes the slope of the shear-thinning curves (on a log-log scale) in the high-shear rate region to change from ~ -0.7 to ~ -1 due to inactivation of the living polymer-like worms. When

increasing the activity this results in a lowering of the zero-shear viscosity, effectively flattening the rheology curve.

To quantitatively understand these results, we first characterize the activity of the living polymers by investigating the dynamics of single worms. Similarly to what one would do for a normal polymer undergoing thermal fluctuations, we quantify the activity of a typical worm by determining the time scale of its shape fluctuations as a function of the level of activity. This is done by taking an image sequence of a single, isolated *Tubifex* worm at various temperatures T. Figures 2(a) and 2(b) show six subsequent images of a typical worm's shape fluctuations in a quasi-two-dimensional space [26] for different levels of activity. Tracking the worm's shape in a concentrated solution is unfortunately technically impossible for us at this moment. However, direct visual observation shows that the worms in an aggregate show a very similar dynamics as isolated worms, notably the dependence on temperature and the effect of alcohol are very similar. We quantify the time-dependent variations in the polymer's end-to-end distance $r_e(t)$ as $\delta r_e(t) = r_e(t) - \langle r_e \rangle_t$.

Figures 2(a) and 2(b) shows typical traces of $\delta r_e(t)$ at high ($T = 30\,^{\circ}\mathrm{C}$) and low activity (addition of alcohol). Next, we calculate the autocorrelation function $g(t) = \langle \delta r_e(t) \delta r_e(t+\tau) \rangle_t / \langle \delta r_e(t)^2 \rangle_t$. The (microscopic) characteristic time of the fluctuations τ_{worm} is then determined from the half-decay time of the autocorrelation function, as shown in Fig. 2(c). We find, as expected, that decreasing the temperature or adding alcohol strongly decreases the activity as quantified by the characteristic time, which increases from 0.26 s at 30 °C to 2.20 s in the presence of alcohol.

We can now quantify the shear thinning for different activities. As shown in Fig. 1, increasing the shear rate is observed to result in a constant-viscosity Newtonian plateau, followed by power-law type shear thinning. Similarly to usual polymer solutions or melts we therefore analyze these results using a classical polymer rheological model based on the Cross equation [34]:

$$\eta_s = \frac{\eta_{s,0}}{1 + (\dot{\gamma}\tau_{\mathrm{rheo}})^{\alpha}}, \tag{1}$$

where $\eta_{s,0}$ is the characteristic zero-shear rate viscosity, τ_{rheo} the average relaxation time (whose inverse corresponds roughly to the onset shear rate for shear thinning) and α the exponent that describes the slope of $\eta_s/\eta_{s,0}$ in the high-shear-rate power-law region; in all cases the exponent n is strictly larger than zero, so that no flow instabilities are anticipated nor observed in our transparent shear cell.

As for thermally activated systems, we find for our active system that τ_{rheo} depends on the activity. As shown in Fig. 2(d), there is a simple linear relation between the relaxation time obtained from rheology experiments (Fig. 1) and the characteristic time of the microscopic conformational fluctuations of an individual worm (Fig. 2); the slower the microscopic dynamics of the worms, the larger the average relaxation time scale of the ensemble of worms. The observation that the macroscopic rheology times are significantly higher than the microscopic times is in agreement with findings for usual polymers: the onset of shear thinning in the rheology is usually assumed to probe the longest relaxation time in the system [35,36]. This is confirmed by performing oscillatory measurements at an intermediate concentration of living polymer-like worms [26]. We find $G' \approx G'' \sim f^{1/2}$, highlighting that multiple relaxation times are present in our material [21]. Perhaps surprisingly for our very complex material, the Cox-Merz rule relating the oscillation to the steady shear experiment seems to hold approximately; this confirms once more the polymer-like nature of our material.

For shear thinning of regular polymers, the usual interpretation of shear thinning is that, for low shear rates, the flow is not fast enough to orient the polymer coils that randomize their orientation due to thermal fluctuations. When the shear rate exceeds the inverse of the characteristic time of these thermal fluctuations, the polymers become oriented and a shear-thinning behaviour is observed. Our worms do not exhibit thermal fluctuations but do perform randomizing fluctuations. The rheology suggests that, to first order, the polymer-like worms behave similarly to classical polymers, with the worms' activity having a similar orientational randomizing effect as thermal fluctuations.

To see how far the similarities with regular polymer extend, we also investigate the effect of the living worm concentration on the shear viscosity for two levels of activity. At low activity [$T = 0\,^{\circ}\mathrm{C}$, Fig. 3(a)], the Cross model is sufficient to describe the flow curves for all concentrations [inset Fig. 3(a)]. These results are at least qualitatively similar to what one would expect for regular (i.e., nonactive) polymers: when the concentration increases, the zero-shear viscosity plateau becomes higher, the onset shear rate for shear thinning smaller and the shear-thinning more pronounced. When the solution is more active [$T = 20\,^{\circ}\mathrm{C}$, Fig. 3(b)], similar trends are observed, but at high shear rates deviations from the simple Cross model become apparent [inset Fig. (b)]. It appears that, in this regime, the interaction between polymer-like worms and the flow is more complicated than for regular polymers: the flow is more efficient at orienting living polymers than conventional ones.

We also observe anomalies in the zero-shear viscosity as a function of the living worm concentration [Fig. 3(c)] for active and nonactive worms. These values are obtained by extrapolation of the experimental low shear rate viscosity using the Cross equation [Eq. (1)]. For regular polymers, the scaling with concentration has been much discussed [37,38]: simple models give a power-law dependence with an exponent around 3 for the increase of the zero-shear viscosity with concentration. Detailed experiments and

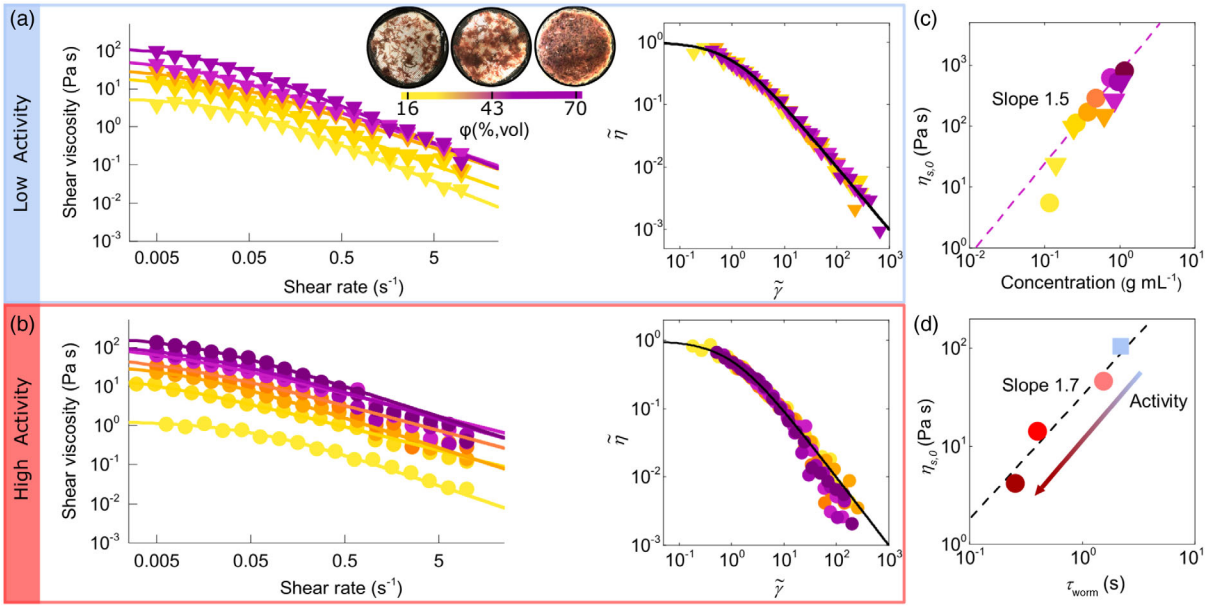

FIG. 3. Effect of the concentration on the polymer-like worm rheology. (a),(b) Shear viscosity as a function of the shear rate for different concentrations of worms in solution at a low [(a): $T = 0\,°\mathrm{C}$] and high [(b): $T = 20\,°\mathrm{C}$] level of activity. Insets: same data as main graph, but normalized by the fitting parameters of the Cross model (continuous lines): $\tilde{\eta} = \eta_s/\eta_{s,0}$ and $\tilde{\dot{\gamma}} = (\dot{\gamma}\tau_{\mathrm{rheo}})^{\alpha}$. The sequence of images shows top views of the container holding typical *Tubifex* solutions at different concentrations from low (yellow, left) to high (purple, right). (c) Zero-shear viscosity $\eta_{s,0}$ as function of living polymer-like concentration at a high level of activity ($T = 20\,°\mathrm{C}$, circles) and low level of activity ($T = 0\,°\mathrm{C}$, triangles). Dashed line has slope 1.5. (d) Effect of activity on the zero-shear viscosity as a function of activity as quantified by the (microscopic) characteristic time of the worms (τ_{worm}) at a polymer concentration $C = 28\%_{\mathrm{vol}}$. Dashed line has slope 1.7.

more sophisticated theories give an exponent that is slightly higher than 3. Our experiments however reveal a much weaker dependence on concentration, with a power-law exponent around 1.5; we interpret this value as an intermediate value between a linear behavior observed for semidilute non-Brownian particle systems and an entangled polymer. In Fig. 3(d) we show that the zero-shear viscosity is also strongly influenced by polymer activity by comparing it to the characteristic time of an individual worm's fluctuations: the lower the activity, the higher the zero-shear viscosity as a an effect of the direct worm-worm interactions [21]. The data suggest a power-law relation between the zero-shear viscosity and τ_{worm}, with an exponent of about 1.7.

Gompper, Winkler, and collaborators [6,7,10] performed an analytical study of the shear thinning of active polymers for a polymer system consisting of active Brownian particles, meaning that each monomer has a random direction of self-propulsion. Interestingly, in the case of large persistence lengths, their model predicts the opposite of what is observed here, namely that increasing the polymers' activity increases the shear thinning. The discrepancy is likely because their analysis is based on the bead-spring model of connected active particles but may not apply to active worm-like chains. Models that consider the polymers to be tangentially driven [5,8,39] appear to be more suitable to our specific system of polymer-like worms. Indeed, some of the qualitative features described in [40] are very similar to the physical behaviour of our worms. For these models, the rheological implications have not been investigated yet. The similarities as well as differences we report between our system of actively driven polymer-like living worms and well-known polymer solutions that undergo thermal fluctuations invite further scrutiny, opening the new research field of "living polymers."

We are very grateful to the three anonymous referees for constructive comments that substantially improved the quality of the Letter. We thank the workshop of the University of Amsterdam for their skilful technical assistance and the Aquarium Holgen for providing fresh batches of *T. Tubifex* worms. A. D. acknowledges the funding from the European Union's Horizon 2020 research and innovation program under the Individual Marie Skłodowska-Curie fellowship Grant Agreement No. 798455.

*A.Deblais@uva.nl
†S.Woutersen@uva.nl
‡D.Bonn@uva.nl

[1] C. Wagner, Y. Amarouchene, D. Bonn, and J. Eggers, Phys. Rev. Lett. **95**, 164504 (2005).
[2] P. LeDuc, C. Haber, G. Bao, and D. Wirtz, Nature (London) **399**, 564 (1999).
[3] A. Perazzo, J. K. Nunes, S. Guido, and H. A. Stone, Proc. Natl. Acad. Sci. U.S.A. **114**, E8557 (2017).

[4] T. B. Liverpool, A. C. Maggs, and A. Ajdari, Phys. Rev. Lett. **86**, 4171 (2001).
[5] M. C. Marchetti, J. F. Joanny, S. Ramaswamy, T. B. Liverpool, J. Prost, M. Rao, and R. A. Simha, Rev. Mod. Phys. **85**, 1143 (2013).
[6] R. G. Winkler, J. Elgeti, and G. Gompper, J. Phys. Soc. Jpn. **86**, 101014 (2017).
[7] A. Martín-Gómez, G. Gompper, and R. G. Winkler, Polymers **10**, 837 (2018).
[8] V. Bianco, E. Locatelli, and P. Malgaretti, Phys. Rev. Lett. **121**, 217802 (2018).
[9] Z. Mokhtari and A. Zippelius, Phys. Rev. Lett. **123**, 028001 (2019).
[10] A. Martín-Gómez, T. Eisenstecken, G. Gompper, and R. G. Winkler, Soft Matter **15**, 3957 (2019).
[11] H.-P. Zhang, A. Be'er, E.-L. Florin, and H. L. Swinney, Proc. Natl. Acad. Sci. U.S.A. **107**, 13626 (2010).
[12] C. Bechinger, R. Di Leonardo, H. Löwen, C. Reichhardt, G. Volpe, and G. Volpe, Rev. Mod. Phys. **88**, 045006 (2016).
[13] J. Schwarz-Linek, C. Valeriani, A. Cacciuto, M. E. Cates, D. Marenduzzo, A. N. Morozov, and W. C. K. Poon, Proc. Natl. Acad. Sci. U.S.A. **109**, 4052 (2012).
[14] É. Fodor and M. Cristina Marchetti, Physica (Amsterdam) **504A**, 106 (2018).
[15] D. T. N. Chen, A. W. C. Lau, L. A. Hough, M. F. Islam, M. Goulian, T. C. Lubensky, and A. G. Yodh, Phys. Rev. Lett. **148302**, 1 (2007).
[16] A. P. Sokolov and K. S. Schweizer, Phys. Rev. Lett. **103**, 148101 (2009).
[17] L. Giomi, T. B. Liverpool, and M. C. Marchetti, Phys. Rev. E **81**, 051908 (2010).
[18] D. L. Koch and G. Subramanian, Annu. Rev. Fluid Mech. **43**, 637 (2011).
[19] E. H. Zhou, F. D. Martinez, and J. J. Fredberg, Nat. Mater. **12**, 184 (2013).
[20] H. M. López, J. Gachelin, C. Douarche, H. Auradou, and E. Clément, Phys. Rev. Lett. **115**, 028301 (2015).
[21] M. Tennenbaum, Z. Liu, D. Hu, and A. Fernandez-nieves, Nat. Mater. **15** (2016).
[22] Y. Hatwalne, S. Ramaswamy, M. Rao, and R. A. Simha, Phys. Rev. Lett. **92**, 118101 (2004).
[23] M. N. van der Linden, L. C. Alexander, D. G. A. L. Aarts, and O. Dauchot, Phys. Rev. Lett. **123**, 098001 (2019).
[24] D. Geyer, D. Martin, J. Tailleur, and D. Bartolo, Phys. Rev. X **9**, 031043 (2019).
[25] M. N. Lazim and M. A. Learner, Ecography **9**, 185 (1986).
[26] See the Supplemental Material at http://link.aps.org/supplemental/10.1103/PhysRevLett.124.188002 for more details on the procedure used to extract the size distribution, diffusion motion and microscopic characteristic timescale describing the individual worm dynamics. It also provides more details on the custom-designed rheology cell used to study the flow behavior of an ensemble of active polymer-like worms in solution. It includes Refs. [25,27,28].
[27] J. G. Walker, Biol. Bull. **140**, 156 (1971).
[28] W. Thielicke and E. Stamhuis, J. Open Res. Software **2**, e30 (2014).
[29] A. Deblais, D. Bonn, and S. Woutersen, arXiv:1912.05951.
[30] V. Groce, T. Cosgrove, and C. A. Dreiss, Langmuir **21**, 6762 (2005).
[31] P. M. McCall, F. C. MacKintosh, D. R. Kovar, and M. L. Gardel, Proc. Natl. Acad. Sci. U.S.A. **116**, 12629 (2019).
[32] A. Fall, N. Huang, F. Bertrand, G. Ovarlez, and D. Bonn, Phys. Rev. Lett. **100**, 018301 (2008).
[33] C. R. Gilbertson and J. D. Wyatt, J. Am. Assoc. Lab. Anim. Sci. **55**, 577 (2016).
[34] R. B. Bird, R. C. Armstrong, and O. Hassager, Dyn. Polym. Liq. **2** (1987).
[35] V. M. Entov and E. J. Hinch, J. Non-Newtonian Fluid Mech. **72**, 31 (1997).
[36] S. L. Anna and G. H. McKinley, J. Rheol. **45**, 115 (2001).
[37] Y. Heo and R. G. Larson, J. Rheol. **49**, 1117 (2005).
[38] J. F. Vega, S. Rastogi, G. W. M. Peters, and H. E. H. Meijer, J. Rheol. **48**, 663 (2004).
[39] R. E. Isele-Holder, J. Elgeti, and G. Gompper, Soft Matter **11**, 7181 (2015).
[40] O. Duman, R. E. Isele-Holder, J. Elgeti, and G. Gompper, Soft Matter **14**, 4483 (2018).